Available online at www.sciencedirect.com
SCIENCE DIRECT
Catalysis Today 99 (2005) 43–49
CATALYSIS TODAY
www.elsevier.com/locate/cattod

Crystalline Mo–V–O based complex oxides as selective oxidation catalysts of propane

Wataru Ueda*, Damien Vitry, Tomokazu Katou

Laboratory of Advanced Material Design, Catalysis Research Center, Hokkaido University, N-21, S-10, Kita-ku, Sapporo 001-0021, Japan

Available online 15 December 2004

Abstract

Three single crystalline Mo–V–O based oxides, Mo–V–O, Mo–V–Te–O and Mo–V–Te–Nb–O, all of which have the same orthorhombic layer-type structure with the particular arrangement of MO_6 (M = Mo, V, Nb) octahedra forming slabs with pentagonal, hexagonal, and heptagonal rings in (1 0 0) plane, were synthesized by hydrothermal method and their catalytic performance in the selective oxidation of propane to acrylic acid were compared in order to elucidate the roles of constituent elements and crystal structure in the course of the propane oxidation. It was observed that the rate of propane oxidation was almost the same over all three catalysts, revealing that Mo and V, which were indispensable elements for the structure formation, were responsible for the catalytic activity for propane oxidation. The Te-containing catalysts showed much higher selectivity to acrylic acid than the Mo–V–O catalyst. Since propene was formed as a main product at low conversion levels over every catalyst, it can be concluded that Te located in the central position of the hexagonal ring promoted the conversion of intermediate propene effectively to acrylic acid. The catalyst with Nb occupying the same structural position of V clearly showed the improved selectively to acrylic acid particularly at high conversion region, because the further oxidation of acrylic acid to CO_x was greatly suppressed. These conclusions were further supported by the additional studies of the determination of activation energy and catalytic oxidations of intermediate products of the propane oxidation.

Keywords: Mo–V–O based complex oxide catalysts; Selective oxidation of propane to acrylic acid; Hydrothermal synthesis; Reaction scheme and the role of constituent elements

1. Introduction

Propane selective oxidation is a recent challenge in the field of catalytic selective oxidation [1,2]. One of the most promising catalysts reported until today is a Mo–V–Te–Nb–O mixed oxide developed by Mitsubishi Chemicals. This catalyst is able to achieve more than 50% of acrylic acid yield per pass [3]. Since then, many of the research on propane oxidation to acrylic acid have been done over this complicated mixed oxide catalyst [4–34]. There are several key issues in the catalyst system: (1) importance of the creation of particular structural phase and relationship between crystal structure and catalytic performance, (2) role of elements constituting the catalysts in relation to the reaction scheme or mechanism, (3) oxidation states of each element on the surface and surface acid–base properties, and (4) surface dynamics and redox property with the involvement of lattice oxide ions in the reaction.

For the first issue, we have demonstrated that the propane oxidation ability of the orthorhombic phase, which assumes a layer-type structure with a particular arrangement of MO_6 (M = Mo, V, Nb) octahedra forming slabs with pentagonal, hexagonal, and heptagonal rings in the (1 0 0) plane (Fig. 1), was superior to that of other related layered materials with different octahedra arrangements in the (1 0 0) plane [35]. This superior activity of the orthorhombic phase of the Mo–V–O based catalysts is highly interesting and suggests the presence of a strong relationship between structure and propane oxidation activity. Then, it has to be clarified why a specific structure is necessary for propane selective oxidation catalysts like the V–P–O catalyst for butane

* Corresponding author. Tel.: +81 11 706 9164; fax: +81 11 706 9163.
E-mail address: ueda@cat.hokudai.ac.jp (W. Ueda).

0920-5861/$ – see front matter © 2004 Elsevier B.V. All rights reserved.
doi:10.1016/j.cattod.2004.09.022

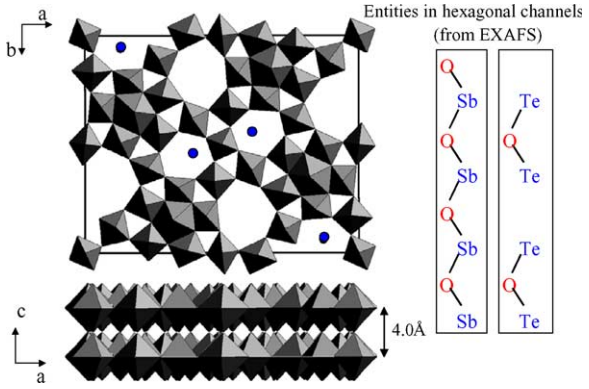

Fig. 1. Structural model of the orthorhombic phase along [0 0 1] and [0 1 0] directions for Mo–V–M–O (M = Sb, Te) oxide catalysts (left part); Mo and V are located in the octahedral positions and in the pentagonal channels and M (M = Te, Sb) is located in hexagonal channels; M entities in hexagonal channels are represented in the left part.

oxidation, while propene oxidation catalysts, so-called mutlicomponent bismuth molybdate catalysts which consist of multi-crystal phase, are not strong structure dependent [36]. Obviously the hardness of propane activation compared to propene must be the main reason for the structure specificity. The best way to access to this point is to elucidate the role of each structural element in the course of propane oxidation to acrylic acid, which is the second issue.

Recently, we have succeeded in preparation of single crystalline Mo–V–O oxide system, Mo–V–O, Mo–V–Te–O, and Mo–V–Te–Nb–O, all of which have the same octahedra framework of the above orthorhombic structure (Fig. 1), by using hydrothermal conditions [37–41]. Since the same structure, the role of each constituent of the catalyst could be deduced by a comparison of oxidation activity of these three catalysts. Here we wish to show details of the hydrothermal preparation of the Mo–V–O based catalysts and to discuss the role on the basis of their catalytic performance.

2. Experimental

Hydrothermal conditions were used for preparing the crystalline Mo–V–O based complex metal oxides. The hydrothermal reaction was carried out at 175 °C for desired duration using a stainless steel autoclave with a Teflon inner tube. All chemicals were used as purchased without any further purification. The detailed preparative procedure of the catalysts is described in the following results and discussion section. The structure of the catalysts was characterized by XRD (Cu Kα) analysis and with Rietveld method. The compositions in each element in the bulk and on the surface were determined by ICP and XPS, respectively. Specific surface area was measured by N_2 adsorption at 77 K using BET method.

Catalytic oxidation in gas-phase was carried out at an atmospheric pressure in a conventional flow system with a fixed bed Pyrex tubular reactor. The feed compositions, the total flow rates of the mixed reactant gases, and the amount of the catalysts used were shown in the footnote of the tables. The reactants and products were analyzed with three on-line gas chromatographs with columns, Molecular Sieve 13X, Gaskuropack 54, and Porapak Q. Carbon balance was always more than 95% but selectivity were calculated on the basis of product sum.

3. Results and discussion

3.1. Preparation of the Mo–V–O based catalysts by hydrothermal method

3.1.1. Preparation of Mo–V–O

An amount of 8.82 g of $(NH_4)_6Mo_7O_{24}{\cdot}4H_2O$ (WAKO Chemicals, 99%) was dissolved in 120 ml of distilled water. Separately, an aqueous solution of vanadium was prepared by dissolving 3.28 g of $VOSO_4{\cdot}nH_2O$ (MITSUWA Chemicals, assay 62%) in 120 ml of distilled water. The two solutions were mixed at 20 °C and stirred for 10 min before being introduced into the stainless steel autoclave equipped with a 300 ml-Teflon inner tube. The concentration of Mo in the mixed solution (dark purple liquid) was 0.2 mol l^{-1}. This concentration parameter was crucial to obtain a well-crystallized sample [40]. Hydrothermal reaction of the liquid (mole ratio: Mo/V = 1/0.25) was carried out for 20 h. Gray solids were yielded in the bottom of the autoclave as well as on the wall. The obtained solid was separated from the solution, washed with distilled water, and dried at 80 °C over night.

The fresh Mo–V–O catalyst had reasonably high uniformity of the particle in which prism-shaped crystals of about 1 μm length were observed by SEM analysis. This crystalline material, which had an elemental composition of $Mo_{1.00}V_{0.34}O_x$ determined by ICP, shows characteristic X-ray diffraction peaks of the orthorhombic structure (6.6°, 7.9°, and 9.0° at angle region lower than 10° and sharp peaks at $2\theta = 22°$ and 45° (Cu Kα)). The XRD pattern was nicely simulated by using orthorhombic structure with lattice parameter ($a = 21.10$ Å, $b = 26.57$ Å, $c = 4.006$ Å). There are many structural variants in Mo–V–O system [42–45] and it is recognized that the structural material synthesized in the present work is a new one. Additionally, it should be pointed out that Te or Sb is unnecessary for the formation of the orthorhombic structure, although it has been thought that the structure formation needs either Te or Sb. The yield of the crystalline material was, however, low (less than 20%) under the present synthetic conditions, presumably due to the difficulty of crystallization of this meta-stable phase without Te or Sb.

After heat-treatment at 500 °C in nitrogen stream (50 ml min^{-1}), the XRD pattern of the crystalline Mo–V–O catalyst was almost unchanged. The surface area was determined to be 6.1 $m^2\ g^{-1}$ by BET. The calcination at

600 °C for 2 h, however, caused the slight decomposition of the catalyst into phases of MoO_3 (JCPDS [76–1003]), $V_{0.95}Mo_{0.97}O_5$ (JCPDS [77–0649]), and $(V_{0.07}Mo_{0.93})_5O_{14}$ (JCPDS [31–1437]).

3.1.2. Preparation of Mo–V–Te–O

In 20 ml of water were successively added 5.35 g of $(NH_4)_6Mo_7O_{24}{\cdot}4H_2O$ (WAKO Chemicals, 99%) and 0.80 g of TeO_2 powder (KATAYAMA Chemicals, 99%). Separately, an aqueous solution of vanadium was prepared by dissolving 3.94 g of $VOSO_4{\cdot}nH_2O$ (MITSUWA Chemicals, assay 62%) in 10 ml of distilled water. The two solutions were mixed at 20 °C and stirred for 10 min before being introduced into the autoclave. After 5 min of nitrogen bubbling for replacing the residual air, the autoclave was sealed and heated for 72 h. Black solid of long rod-shaped crystals with a length of 30–50 μm was obtained and was then washed with distilled water and dried for 12 h at 80 °C. It was first calcined in air at 280 °C for 2 h and then under nitrogen flow (50 ml min^{-1}) at 600 °C for 2 h, as it has been found to be the most effective calcination treatment to give surface area of 6.9 $m^2\ g^{-1}$ and to achieve high acrylic acid selectivity [39]. The XRD pattern of the sample was almost resemble to that of the Mo–V–O catalyst, though peak intensities were slightly different because of Te. All the XRD peaks detected on this sample were able to be indexed with the lattice parameters used for the Mo–V–O catalysts. The structure of this sample was maintained after the calcination even at 600 °C in nitrogen and no additional peaks were detected, which is different from the Mo–V–O sample. The result suggests that Te in the solid stabilizes the structure. The prepared sample had a composition of $Mo_{1.00}V_{0.44}Te_{0.10}O_x$.

3.1.3. Preparation of Mo–V–Te–Nb–O

Koyasu et al. reported several preparation methods of biphasic (orthorhombic and hexagonal) Mo–V–Te–Nb–O catalysts [6,17,26]. We, on the other hand, succeeded in preparing mono-phasic crystalline Mo–V–Te–Nb–O catalyst with the orthorhombic structure [41] by the following procedure. In 20 ml of water heated at 80 °C were successively dissolved 5.35 g of $(NH_4)_6Mo_7O_{24}{\cdot}4H_2O$ (WAKO Chemicals, 99%) and 1.16 g of H_6TeO_6 (KATAYAMA Chemicals, 99%). A second solution was prepared by dissolving 2.37 g of $VOSO_4{\cdot}nH_2O$ (MITSUWA Chemicals, assay 62%) in 10 ml of distilled water. A third solution was simultaneously prepared by dissolving 2.33 g of $Nb_2(C_2O_4)_5{\cdot}nH_2O$ (CBMM, assay 20.5% in Nb_2O_5) in 10 ml of distilled water heated at 80 °C. The solution containing vanadium (the second solution) was then added to the solution containing molybdenum and tellurium and the resulting solution was stirred for 5 min. The solution containing niobium (the third solution) was finally added to the mixed solution and the resulting slurry was stirred for 10 min at 80 °C before being introduced into the autoclave. After 5 min of nitrogen bubbling for replacing the residual air, the autoclave was sealed and heated for 48 h. The dark blue powder obtained was washed with distilled water and dried for 12 h at 80 °C. The Mo–V–Te–Nb–O oxide was calcined under nitrogen flow (50 ml min^{-1}) for 2 h at 600 °C.

The dark blue powder obtained after the hydrothermal synthesis showed a pattern with a few broad XRD peaks, which is completely different from those observed on the fresh Mo–V–O and Mo–V–Te–O sample. The observation of a very broad XRD peak around 22° (indexed to (0 0 1)) indicates that the material seems to be ill-crystallized in the direction of the *c*-axis and disordered in the other axes. Since the main difference in the preparation between the Mo–V–Te–O system and the Mo–V–Te–Nb–O system was whether niobium and oxalate anion are present in the slurry or not, the XRD result indicates that niobium cations and/or oxalate anions retard the crystallization during the hydrothermal synthesis. The crystallization in the Mo–V–Te–Nb–O system occurred only during the calcination in nitrogen at 600 °C as observed by in situ XRD analysis and formed aggregates of small cylinder-shaped crystallites with a length of about 300–500 nm in fine and uniform crystalline size and shape. The XRD pattern of the crystalline structural material formed after the calcination was quite similar to these observed in the case of Mo–V–Te–O and Mo–V–O. The calcined catalyst had a composition of $Mo_{1.00}V_{0.25}Te_{0.11}Nb_{0.12}O_x$ and a surface area of 6.2 $m^2\ g^{-1}$.

3.2. Comparison of catalytic performance of orthorhombic Mo–V–O system

3.2.1. Propane oxidation to acrylic acid

Three catalysts Mo–V–O, Mo–V–Te–O, and Mo–V–Te–Nb–O, were tested in the propane selective oxidation to acrylic acid. The conversions and the product distribution are listed in Table 1 at a reaction temperature of 380 °C which usually gives the best acrylic acid yield per pass. Propane oxidation was carried out at an atmospheric pressure in a conventional flow system with a fixed bed Pyrex tubular reactor. This reaction system was also used for other catalytic oxidations. The reaction conditions were shown in detail in the footnote of the table. The products detected beside acrylic acid were propene, acetic acid, acetone, CO, and CO_2. Other products in this reaction were acrolein, propanol, isopropanol, propionaldehyde, and propionic acid, but all in selectivity less than 1%.

From the results shown in Table 1, it can be first pointed out that three catalysts revealed a similar activity for the propane conversion around 33–36%. The oxygen conversion was, however, lower for the Mo–V–Te–Nb–O catalyst compared to Mo–V–Te–O and Mo–V–O catalysts, simply due to the lower selectivities to CO_x and acetic acid. The second point is that Te enhances the selectivity of acrylic acid drastically (62.4% for the Mo–V–Te–Nb–O catalyst and 46.6% for the Mo–V–Te–O catalyst), since over the Mo–V–O catalyst acrylic acid was detected only in fairly

Table 1
Oxidation of propane over three Mo–V–O based catalysts with the same orthorhombic structure

Catalyst[a]	Reaction temperature (°C)	Conversion[b] of propane (%)	Selectivity[c] (%)					
			AA	C_3H_6	Ace	AcA	CO	CO_2
Mo–V–O	379	32.7	3.4	5.1	0.2	16.9	43.9	30.5
Mo–V–Te–O	380	36.2	46.6	7.7	1.3	16.5	14.3	13.6
Mo–V–Te–Nb–O	380	33.4	62.4	8.7	0.4	7.3	11.1	10.1

[a] Catalyst composition and surface area ($m^2\ g^{-1}$): Mo–V–O; $Mo_{1.00}V_{0.34}O_x$ (6.1), Mo–V–Te–O; $Mo_{1.00}V_{0.44}Te_{0.10}O_x$ (6.9), Mo–V–Te–Nb–O; $Mo_{1.00}V_{0.25}Te_{0.11}Nb_{0.12}O_x$ (6.2).
[b] Reaction conditions: 500 mg catalyst, flow rate; 20 ml min^{-1}, $C_3H_8/O_2/H_2O/N_2$ = 8/10/45/37 mol%.
[c] AA = acrylic acid, Ace = acetone, AcA = acetic acid.

low amount with the main overoxidation products such as CO_x and acetic acid. The third point is that the selectivity to acrylic acid for the Mo–V–Te–Nb–O catalyst was appreciably higher than that for the Mo–V–Te–O catalyst, indicating that the addition of Nb improves the yield of acrylic acid further.

3.2.2. Evolution of catalytic activity for propane oxidation

The result of the first point clearly means that Mo and V in the octahedra framework of the crystalline orthorhombic catalysts are responsible for the oxidation activity for propane. This is further confirmed by the following evidences: (1) It was observed that the propane conversion changed in a quite similar level and trend for all the catalysts as the reaction temperature increased in the 300–380 °C [46,47]. (2) Hence, almost the same values of the apparent activation energy for the propane conversion were obtained for three catalysts, as shown in Table 2. (3) Similar pressure dependencies (about 0.7 order for propane pressure and very low dependency with respect to oxygen pressure) of the propane reaction were also observed (Table 2). This result indicates that the rate-determining step is the oxidative activation of propane on the surface sites where Mo and V are located. It can be easily assumed that propane activated oxidatively converts into propene as an intermediate product. (4) In fact, propene was formed as a main product at low propane conversion levels as can be seen in Fig. 2 where selectivity versus conversion plots are shown for three catalysts. More importantly, the propene selectivity changed virtually in the same manner as the propane conversion increased irrespective of the catalysts. As a summary, the propane oxidation starts by the oxidative activation over Mo and V sites to propene, followed by the consecutive reactions to form acrylic acid.

Although it is unclear at the moment what kind of essential chemistry is involved in the evolution of oxidation activity in the Mo–V–O base catalysts, we speculate the following things. As described above, the orthorhombic Mo–V–O based catalyst is not a simple structural mixture of the phase constructed with the pentagonal ring unit and the phase with the hexagonal ring unit but is a structural material with the additional heptagonal ring. Since neither the Mo–

Table 2
Kinetic parameters of propane oxidation over Mo–V–(Te)–(Nb)–O catalysts

Catalyst[a]	Apparent activation energy[b] (kJ mol^{-1})	Reaction order[c]	
		Propane	O_2
Mo–V–O	68.8	0.7	0.2
Mo–V–Te–O	65.9	0.7	0.1
Mo–V–Te–Nb–O	65.4	0.8	0

The values were for the rate of propane conversion.
[a] Catalyst composition and surface area ($m^2\ g^{-1}$): same as shown in Table 1.
[b] Reaction conditions for propane oxidation: 250 mg catalyst, flow rate; 40 ml min^{-1}, $C_3H_8/O_2/H_2O/N_2$ = 8/10/45/37, temperature range; 300–380 °C.
[c] Reaction conditions for propane oxidation: 250 mg catalyst, flow rate; 40 ml min^{-1}, $C_3H_8/O_2/H_2O/N_2$ = 2.5–20/2.5–20/45/37, reaction temperature; 360 °C.

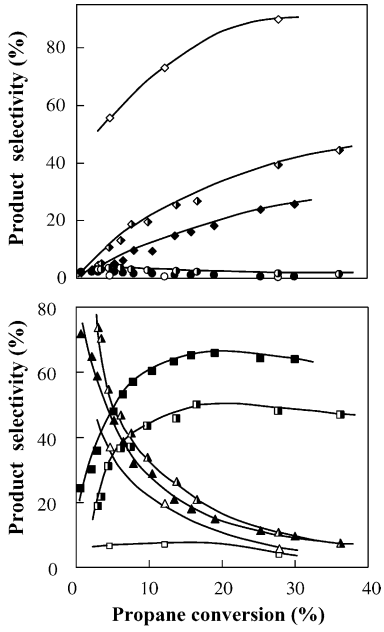

Fig. 2. Selectivity variations of acrylic acid (square), propene (triangle), acetone (circle) and further oxidation products {acetic acid + CO + CO_2} (lozenge) as the function of the propane conversion in the oxidation of propane over Mo–V–O (open mark) and Mo–V–Te–O (semi-closed mark) and Mo–V–Te–Nb–O (closed mark) catalysts at 360 °C. The feed composition was C_3H_8:O_2:N_2:H_2O = 8:10:37:45 (mol%). Amount of the catalysts (from 100 to 500 mg) and the total flow rate (from 20 to 50 ml min^{-1}) were varied for changing the conversion.

V–O catalyst with the pentagonal ring unit only nor one with the hexagonal ring unit only was active for the reaction [48], it is reasonable to assume that the active sites for propane oxidation is generated along with the formation of the heptagonal ring. The point that may relate to the catalytic oxidation activity is concerned about the situation of octahedral coordinations of Mo and V around the heptagonal ring site. We think that the octahedra in the orthorhombic structure must be distorted or puckered when the heptagonal ring is introduced with bringing about the high-dimensional structure, compared to the other relatively simple structural phases which are thus normally symmetric. In fact, a recent report revealed the distortion of the octahedra in the catalysts [34]. Then the Mo and V octahedra may give rise to active oxygen species much easily because of the high distortion, which is suitable for achieving high catalytic activity for oxidation. At the same time, we also think that surface acid site participates in the oxidative activation of propane. The reasons are that the fresh Mo–V–O catalysts synthesized hydrothermally, which contains ammonium cation observable by IR, showed a poor oxidation activity but became active after the removal of ammonium cation by the heat-treatment in N_2 stream, and that the addition of potassium without changing the orthorhombic structure caused the prominent decrease in the oxidation activity. Obviously, further research is necessary for understanding cooperative functions of active oxygen species and surface acid property in the course of the propane oxidative activation.

3.2.3. The roles of Te and Nb in the Mo–V–O based catalysts

First, the second point described above is dealt with, that is, the addition of Te into the Mo–V–O catalyst apparently improved the acrylic acid selectivity without affecting the intrinsic oxidation activity. From a structural point of view, Te seems to have no effect on the oxidation activity of the Mo–V–O framework, because Te occupies the central position of the hexagonal ring unit preferentially with practically no influence on the framework of the Mo and V octahedra. Therefore, the evolution of the selectivity due to Te is the main concern.

Since acrylic acid is formed consecutively after the initial formation of propene over Mo and V sites, as shown in Fig. 2, we carried out the propene oxidation over three catalysts and the results are summarized in Table 3. The propene oxidation took place over the catalysts much faster than the propane oxidation, so that lower reaction temperature, shorter contact time, and lower partial pressure of propene have been chosen for the reaction conditions. Beside acrylic acid, exactly the same side-products as in the propane oxidation were detected. As observed in the propane oxidation, propene was oxidatively converted in a similar extent over the Mo–V–Te–O and Mo–V–Te–Nb–O catalysts, while a reaction temperature of 20 °C higher was needed for the Mo–V–O catalyst to attain a similar propene conversion, indicating the lower activity of the Mo–V–O catalyst in propene oxidation. Here again, the main products detected over Mo–V–O catalyst were CO_x and acetic acid with a total selectivity of nearly 70%, but on the other hand, the acrylic acid selectivity was high from 56% to more than 80% at the expense of further oxidation products as well as acetone formation when Te was incorporated.

All the results confirm that Te is the essential catalytic component promoting the formation of acrylic acid by the oxidation of propene. As Te is a well-known catalytic element for allylic oxidation of olefins, the observed higher activity for propene conversion over the Te-containing catalysts seem to be originated by the rapid allylic-hydrogen abstraction from propene on the Te site to produce acrolein. Therefore, it should be mentioned that the hydrogen abstraction from propane to propene over the Mo and V sites proceed in a different mechanism from that for allylic-hydrogen abstraction over the Te sites.

Table 3
Oxidation of intermediate products over the Mo–V–O based catalysts

Reactant	Catalyst[a]	Reaction temperature (°C)	Conversion[b] of reactant (%)	Selectivity[c] (%)			
				AA	Ace	AcA	CO_x
Propene	Mo–V–O	360	58.0	27.4	6.3	24.6	41.7
	Mo–V–Te–O	342	56.5	55.6	17.3	14.2	12.9
	Mo–V–Te–Nb–O	340	61.1	81.7	6.2	6.7	5.4
Acrolein	Mo–V–O	320	100.0	59.3	0.0	5.6	35.1
	Mo–V–O[d]	230	96.4	94.2	0.0	1.6	4.2
	Mo–V–Te–O	320	100.0	77.2	0.1	3.2	19.5
	Mo–V–Te–Nb–O	320	99.9	88.3	0.1	1.9	9.7
Acrylic acid	Mo–V–O	305	89.2	–	–	13.5	86.5
	Mo–V–Te–O	320	29.4	–	–	21.5	78.5
	Mo–V–Te–Nb–O	320	12.3	–	–	25.7	74.3

[a] Catalyst composition and surface area ($m^2\ g^{-1}$): same as shown in Table 1.

[b] Reaction conditions for propene oxidation: 250 mg catalyst, flow rate; 40 ml min^{-1}, $C_3H_6/O_2/H_2O/N_2$ = 3/10/45/42. Reaction conditions for acrolein oxidation: 250 mg catalyst, flow rate; 50 ml min^{-1}, $C_3H_4O/O_2/H_2O/N_2$ = 0.1/10/45/44.9. Reaction conditions for acrylic acid oxidation: 500 mg catalyst, flow rate; 20 ml min^{-1}, $C_3H_4O_2/O_2/H_2O/N_2$ = 1/10/45/44.

[c] AA = acrylic acid, Ace = acetone, AcA = acetic acid.

[d] Reaction conditions for acrolein oxidation: 450 mg catalyst, flow rate; 111 ml min^{-1}, $C_3H_4O/O_2/H_2O/N_2$ = 4.5/7/25/63.5.

Accordingly, the high selectivity to acrylic acid attained over the Te-containing catalysts appears to be due to that Te provides the reaction pathway from propene to acrylic acid through acrolein. However, for fully understanding the role of Te, it must be considered whether or not Te is necessary for the reaction of acrolein to acrylic acid and for the further reaction of acrylic acid formed. We then conducted the acrolein oxidation and oxidative decomposition of acrylic acid over three catalysts. The results are also summarized in Table 3.

The acrolein oxidation to acrylic acid proceeded very fast and selectively over the catalysts and even the Mo–V–O catalyst gave 95% acrylic acid yield per pass at the temperature as low as 230 °C. The result reveals that Mo and V sites in the crystalline Mo–V–O itself can effectively promote the acrolein oxidation to acrylic acid and Te site is not necessary. This conclusion is not surprising because Mo–V–O based catalysts are well-known to be active for the reaction [48], but the interesting point is that the present crystalline orthorhombic Mo–V–O catalyst is extremely active compared to those reported. The present catalyst, however, became less selective for the formation of acrylic acid, yielding large amounts of acetic acid and CO_x, when the reaction temperature was set higher as applied for the propane oxidation (Table 3). Apparently, the further oxidation of acrylic acid took place largely, and in fact we observed the oxidative decomposition of acrylic acid could occur over the catalysts as listed in Table 3. Interestingly, the extent of the decomposition is greatly dependent of the catalyst; that is, the Mo–V–O catalyst was most active and the Te-containing catalysts showed much less activity. The Nb-containing catalyst was least active. It appears that Te is again a key element for retarding the oxidative decomposition of acrylic acid. We tentatively propose that Te, which has rather basic property compared to the other constituents, can provide an preferential adsorption site for acrylic acid and the formed acrylate on Te is prevented from the further oxidation before the desorption. As a consequence, the Mo–V–O catalyst is principally active for acrylic acid formation in the propane oxidation and Te is necessary to promote the intermediate product as well as stabilize acrylic acid in order to achieve high catalytic performance.

The third point was about the effect of the Nb addition. As already revealed, Nb has no direct effect on the intrinsic oxidation activity of the Mo–V–O based catalyst but has considerable effect on the formation of acrylic acid. In every reaction listed in Tables 1 and 3, the Nb-containing catalyst always achieved higher selectivity to acrylic acid than the other catalysts. The most prominent example is the oxidative decomposition of acrylic acid, clearly indicating that the suppression of the further oxidation is the fundamental role of Nb.

Fig. 2 also shows that the acrylic acid selectivity of the Mo–V–Te–Nb–O catalyst was clearly superior to that of the Mo–V–Te–O catalyst in the region of high propane conversion. However, it should be noted that the superiority of the Mo–V–Te–Nb–O catalysts in terms of product selectivity was not so prominent under low conversion conditions. This means that Nb does not play any fundamental roles in the formation of acrylic acid but does play roles for stabilizing the acrylic acid formed on the catalyst surface and/or for preventing further oxidation by assisting quick desorption.

On the basis of the catalyst characterizations, the following role of Nb can be envisaged in the catalyst for the propane selective oxidation. We think that the role of Nb concerns the stabilization of Te on the catalyst surface. For the catalyst containing Nb, XPS analysis revealed that the surface concentrations of Te and Nb (Mo/V/Te/Nb = 1.00/0.18/0.19/0.17) were richer than the bulk (Mo/V/Te/Nb = 1.00/0.25/0.11/0.12), whereas in the Mo–V–Te–O catalyst, the Te concentration was similar between the catalyst surface (Mo/V/Te = 1.00/0.41/0.11) and in the bulk (Mo/V/Te = 1.00/0.44/0.10). It can be, therefore, assumed that Nb stabilizes Te to be rich on the surface. Te was considered to be a key element in the catalysts for the propene oxidation to acrolein and the stabilization of acrylic acid as we discussed by comparison with the catalytic activity of the Mo–V–O catalyst. Therefore, the enriched surface Te is significant for achieving high selectivity to acrylic acid in the propane selective oxidation. In addition, the oxidation state of Te (probably 6+) may also be stabilized by the addition of Nb, because the zero-order dependency with respect to the oxygen pressure was observed in the propane conversion over the Mo–V–Te–Nb–O catalyst, which means that the activation of molecular oxygen is rapid enough for maintaining a constant oxidation state of the surface.

3.2.4. Reaction mechanism of propane oxidation over multifunctional Mo–V–Te–Nb–O catalysts

It is clear from the above results that acrylic acid is formed by the stepwise oxidation from propane and that selective Mo–V–O based catalysts must have at least four catalytic functions. The first function is to promote the oxidative activation of propane to form propene intermediate via oxidative dehydrogenation; the second one is related to the allylic oxidation of propene to acrolein; the third one concerns the oxidation of acrolein to acrylic acid; and the last one is to provide a suitable adsorption site of acrylic acid. Obviously the first one is most important and difficult, followed by the last and second ones.

Based on the stepwise reaction of propane to acrylic acid [34], we would like to suggest the following reaction model in relation to the catalyst structure with the high-dimensional octahedra framework. Propane molecule is first activated on Mo–O–V–O–H^+ type active sites around the heptagonal ring unit. The next step is the allylic oxidation of propene to acrolein, which occurs on Mo(V)–O–Te–O site around the hexagonal ring unit. Then, acrylic acid is formed by acrolein oxidation over the same Mo–O–V–O–H^+ site as for the first step. The formed acrylic acid adsorbs on Te of the Mo(V)–

O–Te–O site and thus the decomposition of acrylic acid is retarded. This process is assisted by Nb, which is probably located in the pentagonal unit of the structure. This proposed model just emphasizes the importance of the presence of stimulated catalytic functions in a particular structure from the reflection of the complexity of the propane oxidation – more generally speaking, alkane oxidation reaction – to achieve high selectivity in the catalytic oxidation.

4. Conclusions

We described that the organization of catalyst elements and control of the circumstance of each element in a particular structure is highly important for achieving multi-step oxidation like propane oxidation selectively. The reason why this situation happens is that the catalytic oxidation proceeds until a stable product against further oxidation is formed under applied conditions. This means that we are still unable to control the first step of the alkane selective oxidation. In fact, the present work successfully clarified the active elements but not why the catalyst is active, yet. We still have a lot of things that have to be studied in the field of heterogeneous catalytic oxidation.

References

[1] Y. Moro-oka, W. Ueda, Catalysis 6 (1994) 223.
[2] M.M. Lin, Appl. Catal. A 207 (2001) 1.
[3] T. Ushikubo, H. Nakamura, Y. Koyasu, S. Wajiki, US Patent 5,380,933 (1995).
[4] T. Ushikubo, K. Oshima, A. Kayou, M. Vaarkamp, M. Hatano, J. Catal. 169 (1997) 394.
[5] M. Takahashi, S. To, S. Hirose, JP Patent 98,120,617 (1998).
[6] H. Watanabe, Y. Koyasu, Appl. Catal. A 194–195 (2000) 479.
[7] T. Ushikubo, Catal. Today 57 (2000) 331.
[8] M. Lin, T.B. Desai, F.W. Kaiser, P.D. Klugherz, Catal. Today 61 (2000) 223.
[9] T. Shishido, A. Inoue, T. Konishi, I. Matsuura, K. Takehira, Catal. Lett. 68 (2000) 215.
[10] P. Botella, B. Solsona, A. Martinez-Arias, J.M. Lopez Nieto, Catal. Lett. 74 (2001) 149.
[11] S.A. Holmes, J. Al-Saeedi, V.V. Guliants, P. Boolchand, D. Georgiev, U. Hackler, E. Sobkow, Catal. Today 67 (2001) 403.
[12] T. Shishido, T. Konishi, I. Matsuura, Y. Wang, K. Takaki, K. Takehira, Catal. Today 71 (2001) 77.
[13] L. Luo, J.A. Labinger, M.E. Davis, J. Catal. 200 (2001) 222.
[14] M. Aouine, J.L. Dubois, J.M.M. Millet, Chem. Commun. 13 (2001) 1180.
[15] P. Botella, J.M. Lopez Nieto, B. Solsona, Catal. Lett. 78 (2002) 383.
[16] J.M.M. Millet, H. Roussel, A. Pigamo, J.L. Dubois, J.C. Jumas, Appl. Catal. A 232 (2002) 77.
[17] H. Tsuji, Y. Koyasu, J. Am. Chem. Soc. 124 (2002) 5608.
[18] P. Botella, J.M. Lopez Nieto, B. Solsona, A. Misfud, F. Marquez, J. Catal. 209 (2002) 445.
[19] J.N. Al-Saeedi, V.V. Guliants, Appl. Catal. A 237 (2002) 111.
[20] E.K. Novakova, J.C. Vedrine, E.G. Derouane, J. Catal. 211 (2002) 226.
[21] E.K. Novakova, J.C. Vedrine, E.G. Derouane, J. Catal. 211 (2002) 235.
[22] E.K. Novakova, E. Derouane, J.C. Vedrine, Catal. Lett. 83 (2002) 177.
[23] J.M. Lopez Nieto, P. Botella, M.I. Vasquez, A. Dejoz, Chem. Commun. 17 (2002) 1906.
[24] E. Garcia-Gonzalez, J.M. Lopez Nieto, P. Botella, J.M. Gonzalez-Calbet, Chem. Mater. 14 (2002) 4416.
[25] J.N. Al-Saeedi, V.V. Guliants, O. Guerrero-Perez, M.A. Banares, J. Catal. 215 (2003) 108.
[26] H. Tsuji, K. Oshima, Y. Koyasu, Chem. Mater. 15 (2003) 2112.
[27] E. Balcells, F. Borgmeier, I. Grisstede, H.G. Lintz, Catal. Lett. 87 (2003) 195.
[28] J.M. Lopez Nieto, P. Botella, B. Solsona, J.M. Oliver, Catal. Today 81 (2003) 87.
[29] J.C. Vedrine, E.K. Novakova, E.G. Derouane, Catal. Today 81 (2003) 247.
[30] T. Ushikubo, Catal. Today 78 (2003) 79.
[31] J. Holmberg, R.K. Grasselli, A. Andersson, Top. Catal. 23 (2003) 55.
[32] M. Baca, A. Pigamo, J.L. Dubois, J.M.M. Millet, Top. Catal. 23 (2003) 39.
[33] P. DeSanto Jr., D.J. Buttrey, R.K. Grasselli, C.G. Lugmair, A.F. Volpe, B.H. Toby, T. Vogt, Top. Catal. 23 (2003) 23.
[34] R.K. Grasselli, J.D. Burrington, D.J. Buttrey, P. DeSanto Jr., C.G. Lugmair, A.F. Volpe, T. Weingand, Top. Catal. 23 (2003) 5.
[35] D. Vitry, Y. Morikawa, J.L. Dubois, W. Ueda, Top. Catal. 23 (2003) 47.
[36] Y. Moro-oka, W. Ueda, Adv. Catal. 40 (1994) 233.
[37] W. Ueda, K. Oshihara, Appl. Catal. A 200 (2000) 135.
[38] K. Oshihara, T. Hisano, W. Ueda, Top. Catal. 15 (2001) 153.
[39] W. Ueda, K. Oshihara, D. Vitry, T. Hisano, Y. Kayashima, Catal. Survay Asia 6 (2002) 33.
[40] D. Vitry, Y. Morikawa, J.L. Dubois, W. Ueda, Appl. Catal. A 251 (2003) 411.
[41] T. Kato, D. Vitry, W. Ueda, Chem. Lett. 32 (2003) 1028.
[42] H.A. Eick, L. Kihlborg, Acta Chem. Scand. 20 (1966) 722.
[43] L. Kihlborg, Acta Chem. Scand. 21 (1967) 2495.
[44] L. Kihlborg, Acta Chem. Scand. 23 (1969) 1834.
[45] T. Ekstrom, M. Nygren, Acta Chem. Scand. 26 (1972) 1827.
[46] T. Kato, D. Vitry, W. Ueda, Catal. Today 91–92 (2004) 237.
[47] W. Ueda, D. Vitry, T. Kato, Catal. Today 96 (2004) 235.
[48] T.V. Andrushkevich, Catal. Rev. Sci. Eng. 35 (1993) 213.